Density functional theory for the freezing transition of the vortex-line liquid with periodic layer pinning

Xiao Hu,[1] Mengbo Luo,[1,2] and Yuqiang Ma[1,3]
[1]*Computational Materials Science Center, National Institute for Materials Science, Tsukuba 305-0047, Japan*
[2]*Department of Physics, Zhejiang University, Hangzhou 310027, People's Republic of China*
[3]*Department of Physics, Nanjing University, Nanjing 210093, People's Republic of China*
(Received 25 July 2005; revised manuscript received 13 September 2005; published 2 November 2005)

Possible phases and phase transitions of interlayer Josephson vortex lines are explored by the density functional theory. With the aid of liquid correlation functions, the present theory exposes explicitly the interference between the tendency of crystallization driven by the intervortex repulsions and the underlying layer structure. In strong magnetic fields $B \geqslant \sqrt{3}\phi_0/2\gamma s^2$, the freezing transition can be continuous, provided the layer pinning is beyond a threshold value. For magnetic fields around $B=\sqrt{3}\phi_0/8\gamma s^2$, a vortex smectic with more vortices in alternate layers (i.e., period $m=2$) is stabilized by the layer pinning beyond another, larger threshold value; the smectic freezes into lattice via a first-order transition and transforms into liquid via a second-order transition upon temperature sweeping. No thermodynamically stable smectic with period $m \geqslant 3$ can be found even for extremely large layer pinning. In a wide regime of magnetic field, although the layer pinning enhances the lattice order to higher temperatures at commensurate magnetic fields and thus produces a meandering phase boundary in the *H-T* phase diagram, the freezing transition of vortex lattice is one step and first order. In even lower magnetic fields, the effect of layer pinning is small and the phase boundary becomes monotonic, where the anisotropy scaling of the melting line is recovered. Taking material parameters into account, it is found that the $m=2$ smectic is realized in $YBa_2Cu_3O_{7-\delta}$ around $H \simeq 40T$, but not in $Bi_2Sr_2CaCu_2O_{8+y}$. Continuous melting transitions can be observed in $Bi_2Sr_2CaCu_2O_{8+y}$ in magnetic field of several teslas where the Josephson vortex lattice is in the dense limit.

DOI: 10.1103/PhysRevB.72.174503 PACS number(s): 74.25.Dw, 74.25.Qt

It is now well established that the Abrikosov vortex lattice[1] melts via a thermodynamic first-order transition. However, much less consensus has been reached on the interlayer Josephson vortex lattice in spite of considerable efforts. Physics is very rich in the latter case since the layer structure, with which the vortex alignment should be commensurate,[2] breaks partially the *c* axis translational symmetry and the rotational symmetry. As results, the stability of the Josephson vortex lattice can be either enhanced or weakened depending on the normalized magnetic field $\gamma s^2 B/\phi_0$, where $\gamma=\lambda_c/\lambda_{ab}$ is the anisotropy parameter and *s* the layer separation; various Josephson vortex lattices with different orientations compete with each other.[3–7] The proposal of a vortex smectic phase stabilized by the periodic layer pinning and continuous melting transition[8,9] attracted much attention and was followed by many investigations. Recently, sharp drops of resistance were observed in transport experiments conducted in underdoped YBCO samples resembling discontinuous melting,[10] and a first-order melting transition has been found in computer simulations,[11,12] in similar normalized magnetic fields. The discrepancy among these observations probably indicates that the strength of the layer pinning should be examined in more detail. In this aspect, we also notice that experimental phase diagrams for different samples look quite different even after the normalization of magnetic field.[13–15] A full picture that covers both the strong layer pinning regime, where a vortex smectic may be stabilized, and the anisotropy-scaling regime,[13,15,16] is expected.

As a general theory for crystallization, the density functional theory (DFT) was formulated by Ramakrishnan and Yussouff.[17,18] The basic idea is to describe the freezing transition by the direct pair correlation function (DPCF) of liquid, which is related to the structure factor by $S(\mathbf{k}) = 1/[1-\rho_0 C(\mathbf{k})]$. At the clean limit, both the first-order nature of the vortex-liquid freezing and quantitative aspects such as the Lindemann number have been successfully captured by DFT.[19] Later on, DFT was used to investigate vortex systems with point and columnar pinning centers.[20,21]

In view of its advantages, we adopt the DFT to explore the vortex states in the presence of periodic layer pinning. The main results of the present work are summarized as follows. In high magnetic fields where vortices reside in every layer ($m=1$), the freezing transition is found to be continuous when the layer pinning is beyond a threshold value. As the magnetic field decreases, a vortex smectic phase with period $m=2$ is stabilized by layer pinning beyond another (larger) threshold, accompanied by a sequential second- and first-order transitions upon cooling. In low magnetic fields, the effect of layer pinning is suppressed drastically because of the high melting temperature and the large discrepancy between the wavelength of layer pinning and the vortex lattice constant, which naturally recovers the anisotropy scaling of the melting line. It is revealed that the vortex smectic can be observed in $YBa_2Cu_3O_{7-\delta}$ while not in $Bi_2Sr_2CaCu_2O_{8+y}$. Although we concentrate on the vortex system here, the results are available for other systems such as DNA-lipid complexes[22] and two-dimensional boson systems, such as helium4 on substrates and Bose-Einstein condensates (BEC) in optical lattice potential.

Free-energy functional. The total free energy of interlayer

 ©2005 The American Physical Society

Josephson vortices can be separated into two parts.[23–25] The first is of the same form of anisotropic Ginzburg-Landau (GL) theory; the second is the layer pinning energy of individual vortex lines, which breaks the pseudo rotational symmetry and anisotropy scaling property.[16] In the density functional approach,[18,19] the free-energy functional of this system is given by

$$\beta\mathcal{F}[\rho(\mathbf{r})] = \int d^3r\left[\rho(\mathbf{r})\ln\frac{\rho(\mathbf{r})}{\rho_0} + (A-1)\delta\rho(\mathbf{r})\right] - \frac{1}{2}\int d^3r d^3r'\,\delta\rho(\mathbf{r})\delta\rho(\mathbf{r}')C(\mathbf{r}-\mathbf{r}') - \int d^3r\,\delta\rho(\mathbf{r})\beta V_{\mathrm{p}}\cos(qz), \quad (1)$$

where $\delta\rho(\mathbf{r})=\rho(\mathbf{r})-\rho_0$ with $\rho(\mathbf{r})$ the areal vortex density and ρ_0 its average, and $C(\mathbf{r}-\mathbf{r}')$ the DPCF. The magnetic field is along the $\hat{\mathbf{y}}$ direction, and $\hat{\mathbf{z}}$ is along the layer normal. V_{p} is the layer pinning energy per vortex line per unit length, and $q=2\pi/s$.

It is noted that a full expression for the layer pinning includes contributions from higher harmonics $\cos(2n\pi z/s)$ with $n\geqslant 2$.[23] For materials with large anisotropy parameter, such as $Bi_2Sr_2CaCu_2O_{8+y}$ where the correlation length in the c axis is much smaller than the layer separation s, more terms are present than moderately anisotropic materials such as $YBa_2Cu_3O_{7-\delta}$. However, as will become clear in the following discussions, the high harmonics can hardly change the possible phases and phase transitions because of their large wave numbers compared with the reciprocal lattice vectors of Josephson vortex lattice.

The chemical potential A is determined by means of the variational calculus. The free-energy density for a vortex-line lattice, $\rho(\mathbf{r})=\rho_0+\Sigma_{\mathbf{K}}\rho_{\mathbf{K}}\exp(i\mathbf{K}\cdot\mathbf{x})$ with $\mathbf{K}=(K_x,K_z)$ and $K_y=0$ the reciprocal lattice vectors (RLVs), and $\mathbf{x}=(x,z)$, is obtained as

$$\frac{\beta\mathcal{F}}{N_{xz}L_y} = \frac{1}{2\rho_0}\sum_{\mathbf{K}}\rho_{\mathbf{K}}^2 C(\mathbf{K},0) - \ln\int_{\mathrm{u.c.}}\rho_0 dxdz \times\exp\left(\sum_{\mathbf{K}}\rho_{\mathbf{K}}C(\mathbf{K},0)e^{i\mathbf{K}\cdot\mathbf{x}} + \beta V_{\mathrm{p}}\cos(qz)\right), \quad (2)$$

with N_{xz} the number of unit cells (u.c.) and L_y the dimension of the sample along the field direction. The correlation function $C(\mathbf{K},0)=\int d^3rC(\mathbf{r})\exp(-i\mathbf{K}\cdot\mathbf{x})$ is finite because $C(\mathbf{r})$, the liquid correlation function, is short range in the field direction.

The Fourier components of the vortex density $\{\rho_{\mathbf{K}}\}$ serve as the order parameters for the freezing transition. The minimum of free energy is searched numerically in the order-parameter space for candidate lattices for given DPCF and layer pinning energy, which are functions of magnetic field and temperature. From the second term in Eq. (2), crystallization can reduce the total free energy, and the global minimum of free energy is achieved by the lattice phase provided $C(\mathbf{K},0)$ is large enough. While the order-parameter space is of infinite dimensions, order parameters associated with low shells of RLVs of the candidate lattice give correct results in practice.[18,19]

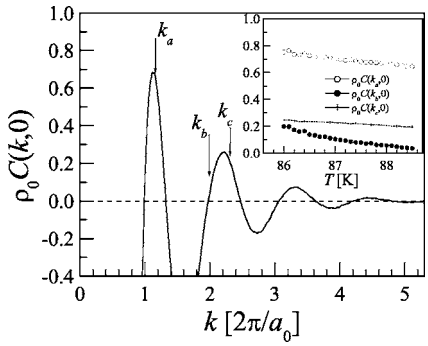

FIG. 1. Typical liquid DPCF $C(k,0)$ for null layer pinning as a function of rescaled wave number k. Inset: temperature dependence of DPCF at three wave numbers k_a, k_b, and k_c corresponding to the first, second, and third shells of RLVs of the equilateral triangular vortex-line lattice. $a_0=\sqrt{2/(\sqrt{3}\rho_0)}$.

DPCF $C(\mathbf{k},0)$. In the present theory, the vortex-liquid DPCF is governed by anisotropic GL theory and *free* of layer pinning. It can be obtained most conveniently by a computer simulation on an *isotropic* vortex system and the anisotropy-scaling treatment $k_x\to\gamma k_x$.[26] Typical rescaled wave-number $(k=\sqrt{(\gamma k_x)^2+k_z^2})$ dependence of the DPCF and temperature dependence at several k values obtained by a computer simulation are displayed in Fig. 1. Due to thermal fluctuations, the DPCF decays quickly with k. The values of DPCF at the primitive, second, and third shell of reciprocal lattice vectors of the triangular vortex lattice can be read from Fig. 1 at k_a, k_b, and k_c, respectively. As shown in the inset of Fig. 1, values of DPCF at reciprocal lattice vectors increase linearly with decreasing temperature. This general property permits one to discuss the phase transition in terms of the correlation function $C(k,0)$ instead of temperature. The absolute value of DPCF $C(k,0)$ decreases with increasing magnetic field since the correlation length in the field direction behaves as $\gamma\sqrt{\phi_0/B}$.[27]

From Eq. (2), the layer pinning enhances the crystallization when q coincides with some RLVs. Since the DPCF $C(\mathbf{K},0)$ decreases quickly with K, this effect is profound when the primitive RLVs $K_z=2\pi/ms$ or those on low shells match q, a situation achieved at high magnetic fields. For weak magnetic fields (thus large m), the pinning energy term decouples from the lattice potential in the second term of Eq. (2) since $q\gg K_z$ and only modifies the measure of the integral slightly. The freezing process is then essentially the same as that of no layer pinning, and the anisotropy scaling property[16] is recovered.[13,15]

Layer pinning energy. When a single vortex line is placed in a periodic layer pinning potential, a kink presumes a metastable state in which a part of the vortex line crosses the pinning barrier and resides in the neighbor energy valley as discussed in Ref. 23. The crossing takes place within the length scale $L_{\mathrm{wall}}\simeq s\sqrt{\gamma\epsilon_0/4U_{\mathrm{p}}}$ (Ref. 9) with $\epsilon_0=(\phi_0/4\pi\lambda_{\mathrm{ab}})^2$ and U_{p},[23]

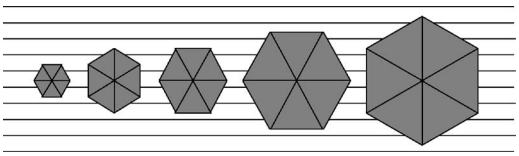

FIG. 2. Josephson vortex lattices commensurate with layer modulation. The x axis is rescaled with the anisotropy parameter γ. The Josephson vortex lattices are labeled in sequence as $A1, B1, A2, A3$, and $B2$, …, where A and B are for the type of unit cell, and the number denotes the c-axis period of vortices in lattice phase in units of layer separation.

$$U_{\mathrm{p}} = 5.23 \times 10^2 \frac{\epsilon_0}{\gamma}\left(\frac{\xi_c}{s}\right)^{5/2} \exp(-15.8\xi_c/s). \tag{3}$$

In the temperature regime where the melting transition occurs, the metastable state is important, and the layer pinning energy is $V_{\mathrm{p}} \simeq s\sqrt{\gamma\epsilon_0 U_{\mathrm{p}}}$ per kink length defined as the separation between two crossings $L_{\mathrm{kink}} = L_{\mathrm{wall}} \exp(2\beta V_{\mathrm{p}})$.[9] This gives the layer pinning strength in free energy (2), where L_y is measured in units of L_{kink}. Numerically, for $YBa_2Cu_3O_{7-\delta}$ with $T_c = 92$ K, $\kappa = 100$, $\gamma = 8$, $\lambda_{ab}(0) = 1000$ Å and $s = 12$ Å, one has $L_{\mathrm{wall}} \simeq 10s$, $L_{\mathrm{kink}} \simeq 60s$, and $\beta V_{\mathrm{p}} \simeq 0.8$ at $T = 88$ K. As temperature decreases, βV_{p} increases linearly to $\beta V_{\mathrm{p}} \simeq 4.3$ at $T = 80K$, L_{wall} decreases slowly and L_{kink} increases exponentially. For $Bi_2Sr_2CaCu_2O_{8+y}$ with $T_c = 90$ K, $\kappa = 100$, $\gamma = 150$, $\lambda_{ab}(0) = 2000$ Å and $s = 15$ Å, one has $\beta V_{\mathrm{p}} \simeq 0.2$ at $T = 84$ K, which increases linearly to $\beta V_{\mathrm{p}} \simeq 0.3$ at $T = 78$ K. In order to seek fully the possible vortex states for various materials, we sweep $\rho_0 C(\mathbf{K}, 0)$ and βV_{p} as they were independent in the following discussions.

Freezing transitions. For high-T_c cuprate superconductors with profound layered structure, it is enough to treat commensurate vortex-line lattice. There are only discrete values of magnetic fields where the vortex-line separation determined by the anisotropic repulsion matches perfectly with the underlying layer structure. Let us begin the DFT analysis with the following set of magnetic fields $B = \sqrt{3}\phi_0/[2\gamma(ms)^2]$, where the *naturally* commensurate vortex lattice is described by the unit vectors $\mathbf{a}_1 = 2\gamma ms/\sqrt{3}\hat{\mathbf{x}}$ and $\mathbf{a}_2 = \gamma ms/\sqrt{3}\hat{\mathbf{x}} + ms\hat{\mathbf{z}}$ with vortices residing m layers away. We call this vortex lattice as Am lattice, as depicted in Fig. 2. The associated unit vectors in reciprocal space are $\mathbf{b}_1 = \sqrt{3}\pi/(\gamma ms)\hat{\mathbf{x}} - \pi/(ms)\hat{\mathbf{z}}$ and $\mathbf{b}_2 = 2\pi/(ms)\hat{\mathbf{z}}$. The layer-pinning wave vector is parallel to the RLVs generated by $\mathbf{b}_2$, which makes enhancement of crystallization due to the layer pinning maximal.

For $m = 1$, one needs at least two order parameters from symmetry, $\rho_{\mathbf{K}1}$ for $\mathbf{K}1 = \mathbf{b}_2$ (and another Bragg spot) and $\rho_{\mathbf{K}2}$ for $\mathbf{K}2 = \mathbf{b}_1$ (and three other Bragg spots). As b_2 coincides with q, $\rho_{\mathbf{K}1}$ is finite even above the freezing temperature, which describes the modulation of vortex density due to layer pinning. Crystallization is signaled by the onset of $\rho_{\mathbf{K}2}$. For small pinning energy, crystallization remains first order, with the freezing point shifting slightly to smaller DPCF and therefore a higher temperature than the case of zero layer pinning. For $\beta V_{\mathrm{p}} \geqslant 0.212$, the freezing becomes continuous. At the *tricritical* layer pinning $\beta V_{\mathrm{p}} = 0.212$, crystallization takes place at $\rho_0 C(k_a, 0) \simeq 0.748$. Similar observations were made by Chakrabarti *et al.* in two-dimensional (2D) colloids under laser radiation,[28] which is not surprising since the crystallization in both systems is governed by the 2D triangular lattice.

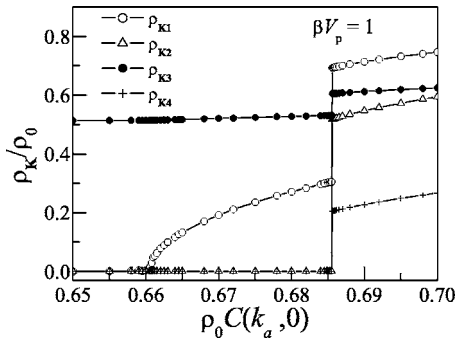

FIG. 3. Two-step freezing of liquid, a second-order transition into an intermediate smectic, and a first-order one into the lattice structure $A2$, upon temperature sweeping. The magnetic field and layer pinning are fixed at $B = \sqrt{3}\phi_0/[2\gamma(ms)^2]$ with $m = 2$ and $\beta V_{\mathrm{p}} = 1$.

For $m = 2$, at least four order parameters $\rho_{\mathbf{K}}$ are necessary where $\mathbf{K}1 = \mathbf{b}_2$, $\mathbf{K}2 = \mathbf{b}_1$, $\mathbf{K}3 = 2\mathbf{b}_2$, and $\mathbf{K}4 = 2\mathbf{b}_1$, with $\rho_{\mathbf{K}3}$ finite even in liquid phase. Freezing transition is first order for low pinning energy. For large pinning energy, a phase characterized by $\rho_{\mathbf{K}1} > 0$ and $\rho_{\mathbf{K}2} = \rho_{\mathbf{K}4} = 0$ appears from liquid via a second-order phase transition as shown in Fig. 3 for $\beta V_{\mathrm{p}} = 1$. The vortex-density modulation is associated with a wave number half of q, with more vortices residing in every other layer. Since the order parameters associated with reciprocal vectors of finite $\hat{\mathbf{x}}$ components are vanishing, the system behaves as liquid in the $\hat{\mathbf{x}}$ direction. This is the smectic order proposed in Ref. 9. As DPCF increases, the full lattice order turns on via a first-order transition. The $\rho_0 C(k_a, 0) - \beta V_{\mathrm{p}}$ phase diagram for $B = \sqrt{3}\phi_0/(8\gamma s^2)$ is presented in Fig. 4, with a multicritical point at $\rho_0 C(k_a, 0) \simeq 0.714$ and $\beta V_{\mathrm{p}} \simeq 0.712$.

Since the liquid-smectic transition is continuous, one can expand the free energy Eq. (2) per vortex per length L_{kink} in terms of the order parameter $\rho_{\pm\mathbf{K}1}$ around the transition point,

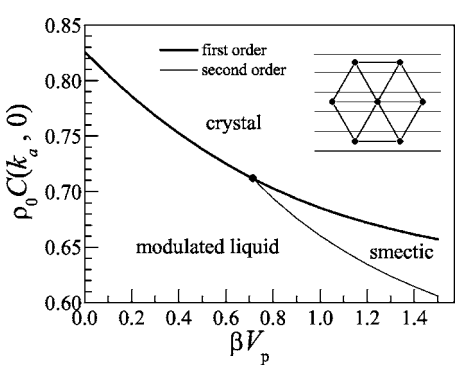

FIG. 4. $\rho_0 C(k_a, 0) - \beta V_{\mathrm{p}}$ phase diagram for $B = \sqrt{3}\phi_0/[2\gamma(ms)^2]$ with $m = 2$.

$$\beta f = -\ln p_0 + \left(\frac{\rho_K}{\rho_0}\right)^2 \rho_0 C(K,0)\left(1 - \frac{2p_2}{p_0}\rho_0 C(K,0)\right) + \left(\frac{\rho_K}{\rho_0}\right)^4 [\rho_0 C(K,0)]^4 \left(2\left(\frac{p_2}{p_0}\right)^2 - \frac{2p_4}{3p_0}\right) + \cdots, \quad (4)$$

with

$$p_n = \int_0^{2s} \frac{dz}{2s} \cos^n(Kz)\exp[\beta V_p \cos(2Kz)], \quad (5)$$

where $K=\pi/s$. The transition point is given by the zero of the second term. The DFT thus derives explicitly the coefficients of Landau free-energy expansion in terms of the DPCF $C(K,0)$, which contains many-body correlations around the transition point, and the layer pinning βV_p. The correlation lengths in the z and y directions diverge as temperature approaches the smectic transition point.

On a more basic level, thermal fluctuations in the vortex density are described in terms of displacements of vortices as

$$\rho(\mathbf{r}) - \rho_0 = \rho_{\mathbf{K}1} \exp(-i\mathbf{K}1\cdot\mathbf{u})\exp(i\mathbf{K}1\cdot\mathbf{r}) + \text{c.c.}, \quad (6)$$

with $\mathbf{u}\equiv\mathbf{u}(\mathbf{r})=u_z(y,z)\hat{\mathbf{z}}$ the displacement field in the z direction. The layer structure of cuprates confines the displacement to $u_z(y,z)=0$ and $\pm s$, which makes $\exp(-i\mathbf{K}1\cdot\mathbf{u})=\pm 1$ and thus real-number order parameters $\pm\rho_K$ as in Eqs. (2) and (4). Therefore, the critical phenomena of the present smectic transition fall into the 2D Ising universality class,[9] where correlations of displacement fields become long range in the y and z directions, while those in x direction remain short range (see Fig. 3). It is noticed that the Landau-Peierls instability observed in smectic transitions of liquid crystal[29,30] is removed by the layer structure of cuprates, namely $u_z(y,z)=0,\pm s$, and that the smectic order in the present system is a genuine long-range order. This makes the DFT, and the Landau theory Eq. (4), to be able to grasp the essence of the phase transition except for critical exponents, as is well known. The logarithmic divergence in the specific heat in the 2D Ising class may be helpful in experimental searches for this smectic phase.

For $m\geqslant 3$, one cannot find a stable smectic phase even for extremely large layer pinning strength. Physically it is because the wave number of the layer pinning is too large to stabilize a smectic characterized by fluctuations of small wave numbers given by the (low) magnetic field. One might argue that, as in Eq. (2), the layer pinning should play a role through the RLVs in higher shells which possess the same wave number as the layer pinning. However, it is found that for $m=3$ the correlation function $C(2\pi/s,0)$, with which the layer pinning plays a role if any, is suppressed significantly by thermal fluctuations as $C(2\pi/s,0)\simeq C(2\pi/3s,0)/15$, where $2\pi/3s$ is the wave number of the $m=3$ smectic order. This tendency becomes more serious for larger m and thus lower magnetic fields.

For magnetic fields $B=\phi_0/[2\sqrt{3}\gamma(ms)^2]$, naturally commensurate vortex lattices of unit vectors $\mathbf{a}_1=2ms\hat{\mathbf{z}}$ and $\mathbf{a}_2=\sqrt{3}\gamma ms\hat{\mathbf{x}}+ms\hat{\mathbf{z}}$, defined as Bm lattice in Fig. 2, are realized with vortices residing m layers away, and unit vectors in reciprocal space $\mathbf{b}_1=-\pi/(\sqrt{3}\gamma ms)\hat{\mathbf{x}}+\pi/(ms)\hat{\mathbf{z}}$ and $\mathbf{b}_2=2\pi/(\sqrt{3}\gamma ms)\hat{\mathbf{x}}$. It is clear that for this lattice orientation none of the six principle RLVs is parallel to the wave vector of layer pinning. Although quantitative enhancement of crystallization by the layer pinning is found, the freezing transition is first order where all the six primitive Bragg peaks appear simultaneously.

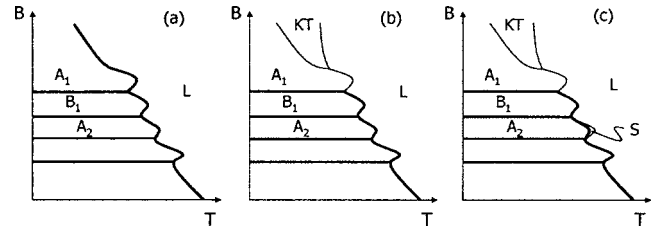

FIG. 5. Possible B-T phase diagrams for materials of (a) weak, (b) moderate, and (c) strong layer pinning. L, S, and KT abbreviate liquid, smectic, and Kosterlitz-Thouless phases, respectively, and $A1$, $B1$ and $A2$ for lattices with specified structures. The thick (thin) curves denote first-order (continuous) phase boundaries. The intermediate phase at the highest magnetic fields refers to the KT phase found in computer simulations.[12] The enhancement of the melting temperature at commensurate magnetic fields is only schematic and not to scale.

There are naturally commensurate vortex lattices with unit vectors neither parallel (as in A type) nor perpendicular (as in B type) to the layer structure. An example is given by unit vectors $\mathbf{a}_1=-\gamma s/\sqrt{3}\hat{\mathbf{x}}+3s\hat{\mathbf{z}}$ and $\mathbf{a}_2=4\gamma/\sqrt{3}s\hat{\mathbf{x}}+2s\hat{\mathbf{z}}$ achieved at $B=\sqrt{3}\phi_0/(14\gamma s^2)$ with vortex lines residing in every layer.[7] Since there is no RLV of this vortex lattice compatible with the layer pinning, the freezing transition is single and first order as discussed above.

For other magnetic fields, vortex lattices are realized by adjusting the x-axis lattice constant from those discussed above. Properties of the naturally commensurate magnetic fields persist to certain extents of field deviation. Freezing temperature, however, drops since the peak values of the DPCF's (see Fig. 1) are not available anymore for the distorted vortex lattices. This causes a meandering melting line in the phase diagram.[9,13] When the RLVs of a distorted vortex-line lattice fall in the wave-number window of negative $C(k,0)$, layer pinning generates strong frustrations to the vortex alignment, which can make the freezing temperature even lower than that of zero layer pinning. The DFT describes first-order transitions between different vortex lattices by comparing their free energies.[3,5–7]

Phase diagram. Possible topologies of B-T phase diagram can be figured out based on the above analyses. Figure 5(a) corresponds to systems of weak layer pinning, in which freezing is always first order. The (almost) flat phase boundaries are between different vortex lattices such as $A1$, $B1$, and $A2$, and so on.[3–7] In Fig. 5(b), the freezing transition into vortex lattice $A1$ is continuous in high magnetic fields where the freezing temperature is low and the layer pinning is beyond $\beta V_p=0.212$. For materials of even stronger layer pinning $\beta V_p\geqslant 0.712$ around $B=\sqrt{3}\phi_0/(8\gamma s^2)$, an $m=2$ smectic phase appears and transforms into lattice $A2$ upon cooling as shown in Fig. 5(c). The Kosterlitz-Thouless (KT) phase in

the high magnetic-field limit found in computer simulations[12] is also included (for details see the discussion below). No further complex topology of phase diagram is expected from DFT.

Taking into account the material parameters, we expect that the B-T phase diagram of $YBa_2Cu_3O_{7-\delta}$ corresponds to Fig. 5(c). Explicitly, an $m=2$ smectic phase is possible around $B \simeq 40T$ taking $\gamma=8$,[8,15] a magnetic field available in laboratory now. The material $Bi_2Sr_2CaCu_2O_{8+y}$ is expected to exhibit the phase diagram in Fig. 5(b). Namely, while the layer pinning is not sufficient to stabilize the smectic, continuous freezing transition(s) into the $A1$ lattice should be accessible above $B=\sqrt{3}\phi_0/(2\gamma s^2) \simeq 5$ T presuming $\gamma=150$.

Discussions. We compare successfully the results of DFT with those by computer simulations based on the frustrated XY model.[12] The first-order melting transition observed in Monte Carlo simulations for $B=\phi_0/32s^2$ and $\gamma=8$ (Refs. 11 and 12) is in accordance with the DFT, since these parameters generate a vortex lattice of $B1$ type with x lattice constant slightly stretched from the naturally commensurate $B1$ lattice.

The continuous melting transitions found by computer simulations for $B=\phi_0/32s^2$ and $\gamma=20$ (Ref. 12), whose ground state is an $A1$-type vortex lattice, are also compatible with DFT, which predicts the melting to be continuous (for $\beta V_p \geqslant 0.212$). Attentions should be paid to DFT in order to see the true critical phenomena at the strong field limit, where the $A1$-type lattice is the ground state, since generally the order parameter is not a real number in contrast with the cases of first-order transitions and the smectic transition discussed above. Explicitly, one has

$$\rho(\mathbf{r}) - \rho_0 = \rho_{\mathbf{K}_1} \exp(i\mathbf{K}_1 \cdot \mathbf{r}) + \Psi_2 \exp(i\mathbf{K}_2 \cdot \mathbf{r}) + \Psi_3 \exp(i\mathbf{K}_3 \cdot \mathbf{r}) + \text{c.c.}, \tag{7}$$

with $\mathbf{K}_1=2\pi/s\hat{\mathbf{z}}, \mathbf{K}_{2,3}=\pm 2\pi f/s\hat{\mathbf{x}} - \pi/s\hat{\mathbf{z}}$ and $\Psi_{2,3} = |\Psi| \exp(-i\mathbf{K}_{2,3}\cdot\mathbf{u})$, for $f \equiv Bs^2/\phi_0$ down to slightly below $f_1=\sqrt{3}/2\gamma$, i.e., magnetic induction down to slightly below the commensurate value $B=\sqrt{3}\phi_0/2\gamma s^2$, such that the ground state is an $A1$-type vortex lattice. In the strong magnetic-field limit, the profound layer structure of the cuprates establishes a strong but trivial order with $\rho_{\mathbf{K}_1} \sim 1$ and the displacement field $\mathbf{u} \equiv \mathbf{u}(\mathbf{r}) = u_x(\mathbf{r})\hat{\mathbf{x}}$. Therefore, the true order parameter is $\Psi_{2,3}=|\Psi|\exp(\mp i2\pi f u_x/\mathrm{s})$.

The mean-field, continuous phase transition in DFT associated with the onset of $|\Psi|$ is suppressed by thermal fluctuations to a crossover, while the true phase transition occurs at lower temperatures, which should be described by $\Psi_{2,3}$ with the $U(1)$ symmetry (i.e., u_x is of modulus of the lattice constant in the x direction s/f). There are two possibilities concerning the critical fluctuations: (i) correlations among the displacement fields grow into long range simultaneously in three directions; (ii) correlations among displacement fields become (quasi) long range first in x and y directions while those in the z direction remain short range at an upper critical temperature, and then grow into long range in all three directions at a lower one. In the first case, the melting transition is single and in the universality class of the three-dimensional (3D) XY model. In the second case, we experience sequentially KT and 3D XY transitions, with an intermediate KT phase, as revealed in the computer simulations.[12] The intermediate KT phase is included in the phase diagrams Figs. 5(b) and 5(c). [A very recent experiment conducted in single crystal of $Bi_2Sr_2CaCu_2O_{8+y}$ supports the phase diagram in Fig. 5(b).[31]] Computer simulations treat thermal fluctuations better than DFT when the structure of vortex lattice is easy to figure out, such as at the strong limit of magnetic field. On the other hand, DFT has its advantage in treating various competing vortex lattices in moderate and weak magnetic fields.

As revealed in the present study, the smectic is stabilized only for magnetic fields in the regime where the ground state is the $A2$-type vortex lattice. For magnetic fields where, for example, the $B1$ vortex lattice becomes the ground state, although the layer pinning cannot generate a stable smectic, it does enhance the lattice order to a higher temperature. Therefore, in spite of that the melting transition of $B1$-type Josephson vortex lattice is qualitatively the same as the Abrikosov vortex lattice, anisotropy scaling on the melting line[16] does not apply around this magnetic field. The scaling property is recovered only for magnetic fields below that of the $A3$ vortex lattice, where the melting line is monotonic. The reason is twofold: first, as seen in Eq. (3) the layer pinning is weak since the c-axis correlation length becomes larger than the layer separation when the melting temperature approaches the zero-field critical point; secondly, the effect of the layer pinning is suppressed by thermal fluctuations significantly, even if an artificially large layer pinning was assumed, since a large discrepancy exists between the wave number of layer pinning and the reciprocal lattice vector of Josephson vortex lattice.

One may expect that the results derived above apply to 2D classical systems[18] with periodic line pinning. It is noticed however that thermal fluctuations are more important in 2D as addressed in Ref. 32.

The authors are grateful to M. Tachiki, L. Bulaevskii, A. Koshelev, W. Kwok, U. Welp, and V. Vinokur for useful discussions, and to V. M. Krasnov for helpful communications. This work was partially supported by Japan Society for the Promotion of Science [Grant-in-Aid for Scientific Research (C) No. 15540355].

[1] A. A. Abrikosov, Zh. Eksp. Teor. Fiz. **32**, 1442 (1957) [Sov. Phys. JETP **5**, 1174 (1957)].
[2] M. Tachiki and S. Takahashi, Solid State Commun. **70**, 291 (1989).
[3] L. J. Campbell, M. M. Doria, and V. G. Kogan, Phys. Rev. B **38**, 2439 (1988).
[4] B. I. Ivlev, N. B. Kopnin, and V. L. Pokrovsky, J. Low Temp. Phys. **80**, 187 (1990).
[5] L. Bulaevskii and J. R. Clem, Phys. Rev. B **44**, 10234 (1991).
[6] M. Ichioka, Phys. Rev. B **51**, R9423 (1995).
[7] A. Koshelev (private communication).
[8] W. K. Kwok, J. Fendrich, U. Welp, S. Fleshler, J. Downey, and G. W. Crabtree, Phys. Rev. Lett. **72**, 1088 (1994).
[9] L. Balents and D. R. Nelson, Phys. Rev. B **52**, 12951 (1995).
[10] M. Andersson, B. Lundqvist, and O. Rapp, Physica C **388-389**, 691 (2003).
[11] X. Hu and M. Tachiki, Phys. Rev. Lett. **85**, 2577 (2000).
[12] X. Hu and M. Tachiki, Phys. Rev. B **70**, 064506 (2004).
[13] S. N. Gordeev, A. A. Zhukov, P. A. J. de Groot, A. G. M. Jansen, R. Gagnon, and L. Taillefer, Phys. Rev. Lett. **85**, 4594 (2000).
[14] B. Lundqvist, O. Rapp, M. Andersson, and Y. Eltsev, Phys. Rev. B **64**, 060503(R) (2001).
[15] A. Schilling, U. Welp, W. K. Kwok, and G. W. Crabtree, Phys. Rev. B **65**, 054505 (2002).
[16] G. Blatter, V. B. Geshkenbein, and A. I. Larkin, Phys. Rev. Lett. **68**, 875 (1992).
[17] T. V. Ramakrishnan and M. Yussouff, Phys. Rev. B **19**, 2775 (1979).
[18] T. V. Ramakrishnan, Phys. Rev. Lett. **48**, 541 (1982).
[19] S. Sengupta, C. Dasgupta, H. R. Krishnamurthy, G. I. Menon, and T. V. Ramakrishnan, Phys. Rev. Lett. **67**, 3444 (1991); I. F. Herbut and Z. Tešanović, *ibid.* **73**, 484 (1994); G. I. Menon, C. Dasgupta, H. R. Krishnamurthy, T. V. Ramakrishnan, and S. Sengupta, Phys. Rev. B **54**, 16192 (1996).
[20] G. I. Menon and C. Dasgupta, Phys. Rev. Lett. **73**, 1023 (1994).
[21] C. Dasgupta and O. T. Valls, Phys. Rev. Lett. **87**, 257002 (2001); Phys. Rev. B **66**, 064518 (2002).
[22] C. S. O'Hern and T. C. Lubensky, Phys. Rev. Lett. **80**, 4345 (1998).
[23] A. Barone, A. I. Larkin, and Y. N. Ovchinnikov, J. Supercond. **3**, 155 (1990).
[24] J. R. Clem and M. W. Coffey, Phys. Rev. B **42**, 6209 (1990).
[25] V. M. Krasnov, Phys. Rev. B **63**, 064519 (2001).
[26] Computer simulations for deriving liquid properties of an isotropic system without layer pinning is much easier than to simulate directly the melting transition of an anisotropic system in presence of layer pinning (Refs. 11 and 12). Details will be presented elsewhere.
[27] J. Kierfeld and V. Vinokur, Phys. Rev. B **69**, 024501 (2004), and references therein.
[28] J. Chakrabarti, H. R. Krishnamurthy, and A. K. Sood, Phys. Rev. Lett. **73**, 2923 (1994).
[29] L. D. Landau, in *Collected Papers of L. D. Landau*, edited by D. Ter Haar (Gordon and Breach, New York, 1965), p. 209.
[30] R. E. Peierls, Helv. Phys. Acta **7**, Suppl., 81 (1934).
[31] Yu. I. Latyshev, V. N. Pavlenko, A. P. Orlov, and X. Hu, JETP Lett. **82**, 232 (2005).
[32] E. Frey, D. R. Nelson, and L. Radzihovsky, Phys. Rev. Lett. **83**, 2977 (1999).